Article

Neighboring-Pixel-Based Maximum Power Point Tracking Algorithm for Partially Shaded Photovoltaic (PV) Systems

Huma Rehman [1], Ali Faisal Murtaza [1], Hadeed Ahmed Sher [2,*], Abdullah M. Noman [3], Abdullrahman A. Al-Shamma'a [3], Abdulaziz Alkuhayli [3] and Filippo Spertino [4]

1   Faculty of Engineering, University of Central Punjab (UCP), Lahore 54782, Pakistan;
    humarehmanbaig@gmail.com (H.R.); ali.faisal@ucp.edu.pk (A.F.M.)
2   Faculty of Electrical Engineering, Ghulam Ishaq Khan Institute of Engineering Sciences and Technology,
    Topi 23460, Pakistan
3   Electrical Engineering Department, College of Engineering, King Saud University,
    Riyadh 11421, Saudi Arabia; anoman@ksu.edu.sa (A.M.N.); ashammaa@ksu.edu.sa (A.A.A.-S.);
    aalkuhayli@ksu.edu.sa (A.A.)
4   Dipartimento Energia "Galileo Ferraris", Politecnico di Torino, Corso Duca degli Abruzzi 24,
    10129 Torino, Italy; filippo.spertino@polito.it
*   Correspondence: hadeedsher@gmail.com

Abstract: In this paper, a neighboring-pixel-based virtual imaging (NPBVI) technique is developed to comprehensively detect the shading conditions on PV arrays. The proposed VI technique is then merged with a probabilistic mechanism of shaded module currents. Finally, a mathematical model is presented, which predicts the current voltage (I-V) region corresponding to the global maximum (GM) of the shaded PV array. The effectiveness of the proposed NPBVI MPPT is validated through numerous experiments that were carried out using a hardware prototype with a 150 W power rating. For the experiments, a PV array consisting of 3×2 ($N_p \times N_s$) 20 W PV modules was utilized. The experiments showcase agreement that the proposed method successfully identified the GM region of a partially shaded PV array.

Keywords: MPPT; virtual Imaging techniques; image processing; photovoltaic systems; partial shading

1. Introduction

Photovoltaic energy systems are some of the cleanest sources of energy among all renewable energy sources, as they are non-contaminating and have low maintenance costs [1–3]. The PV modules are usually connected in series/parallel connection to form a PV array that can fulfill the requirements of a reasonable domestic load. The current–voltage (I-V) and power–voltage (P-V) characteristics of a PV array are discrete under homogeneous irradiation conditions and, hence, demonstrate a distinguishable maximum power point (MPP) [4,5].

It is the instinctive but inescapable phenomenon of partial shade under which PV arrays demonstrate numerous local maxima (LM) points as shown in Figure 1. The I-V P-V characteristics of a PV system are nonlinear with respect to the solar irradiance, load impedance and temperature of a PV cell [6].

Several MPPT algorithms and hardware techniques have been proposed in the literature for tracking the maximum power from a PV system under partial shade [7–10]. Traditional techniques for tracking the MPP of a PV array either strive for oscillations around the MPP (the hill climbing method) or involve techniques that are very computationally intricate (artificial-intelligence-based techniques). Moreover, these techniques demand complete scanning of I-V/P-V curves in order to achieve the MPP [11].
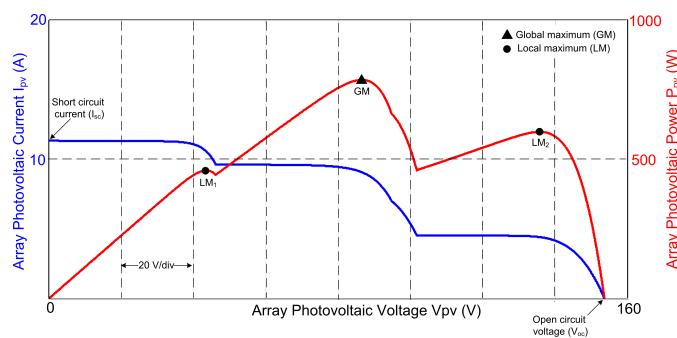
Figure 1. Characteristic curve of an arbitrary PV array under partial shade conditions.

The trend of employing the virtual imaging technique (VIT) for MPPT has soared in the recent past. Due to the major benefit of a non-intrusive electronic interface circuit, the VIT has attracted many researchers to work in this field. In [12], the dust accumulation on a PV array was detected for a PV-array-cleaning robot. In [13], thermal imaging was adopted to detect micro cracks in PV cells. The application of VI is not only limited to condition or performance monitoring of PV arrays but is also used in MPPT as well.

For example, in [14], the authors used the concept of thermography to detect partially shaded modules in a PV array. This method detects partial shading through the differential temperature between a healthy and an unhealthy module of the PV array. It does not require scanning the I-V/P-V curves but instead takes into account the phenomenon of temperature in spite of the irradiance that is directly affecting the current.

Moreover, this technique [14] becomes limited if partial shading occurs on more than one module of a PV array at a time. In [15], a similar technique was proposed, based on the analysis of a single cell of a PV panel. In [16], the maximum power point tracking of a PV array is performed by shadow detection using a video camera and subsequent canny edge detection and image morphology based processing. Based on this, the algorithm reconfigures a PV array to mitigate the partial shading effects [16].

This technique is unable to distinguish between light shade and dark shade. The nature of shade impacts the current produced by the module. Thus, the information about the intensity of shading is significant for the precise operation of the MPP tracker. In [17], the partial shading of a PV module was detected using an optical camera. In [18], an aerial drone was used to visualize the condition of a large PV field. However, this may not be feasible for small PV applications. Infrared imaging was used to detect aging in [19,20]. This work, although not related to the MPPT, provides a useful insight about the use of cameras for PV systems.

Our paper presents a method to detect the global maxima (GM) of partially shaded PV array using a virtual imaging technique. The proposed technique to acquire images of a PV array uses a simple optical camera and is able to distinguish between light and dark shade conditions. Unlike existing techniques, the proposed technique is independent of the factor of temperature, which is affected by the natural phenomenon of partial shading. However, temperature is a time-dependent phenomenon, and thus it might introduce a delay in the processing of an MPP tracker.

Once the proposed technique discovers the partially shaded module in the PV array, this visual information is further transformed into I-V parametric equations that are solved in order to find the maximum power point region under that particular shading scenario. Furthermore, the proposed method is mathematically less complex due to the fewer mathematical operations that are involved.

The rest of the paper is as follows. Section 2 describes the workflow for virtual imaging. This section also includes the image formulation model based on existing techniques and the proposed neighboring-pixel-based algorithm. Section 3 details the validation of the proposed NPBVI MPPT. The sizing of the PV array and the design parameters of the DC-DC converter are also explained in Section 3. The paper concludes with Section 4.

2. Proposed MPPT

2.1. The Image Formation Model

Images are usually denoted in two dimensions of the form $f(x, y)$, which is a positive scalar quantity. The physical value of this function is determined by the source of the image. An image is generated in a way that the image intensity value is proportional to the energy radiated by a physical source [21]. Consequently, the mathematical form of image $f(x, y)$ has a non-zero finite value as expressed in Equation (1)

$$0 < f(x, y) < \infty \tag{1}$$

The function expressed in (1) is signaled by two components: (1) the light that is incident on the object being viewed, known as the illumination; and (2) the illumination reflected by the object, known as the reflectance. The illumination $(i(x, y))$ and reflectance $(r(x, y))$ can mathematically be described as (2)

$$
\begin{aligned}
f(x, y) &= i(x, y) r(x, y) \\
&\textit{Where,} \\
0 &< i(x, y) < \infty \\
&\textit{and} \\
0 &< r(x, y) < 1
\end{aligned}
\tag{2}
$$

The nature of $i(x, y)$ is determined by the illumination source, which is the sun in the case of PV and MPPT, and that of $r(x, y)$ is determined by the characteristics of the object, which is the PV module in this manuscript. The image is then converted into digital form using sampling and quantization so that the function $f(x, y)$ is sampled in terms of the coordinates and amplitude. The process of digitizing the coordinate values of the function is termed as sampling, while digitizing the amplitude value is known as quantization.

2.2. Existing Image Processing Techniques

In this proposed work, the shade on a PV panel is detected using the built-in libraries of MATLAB [22]. In this regard, several image processing techniques, e.g., Canny/Sobel Edge detection, image morphology (dilation, erosion), and black & white images were tested as shown in Figure 2. During the validation process, we noticed that, in all these MATLAB imaging techniques, useful shadow information was either lost or over-written. Moreover, these techniques were not capable of differentiating between a partially shaded and a fully shaded PV module. It is also well established that the pattern of shade directly impacts the output power of the PV module [8,23–25].
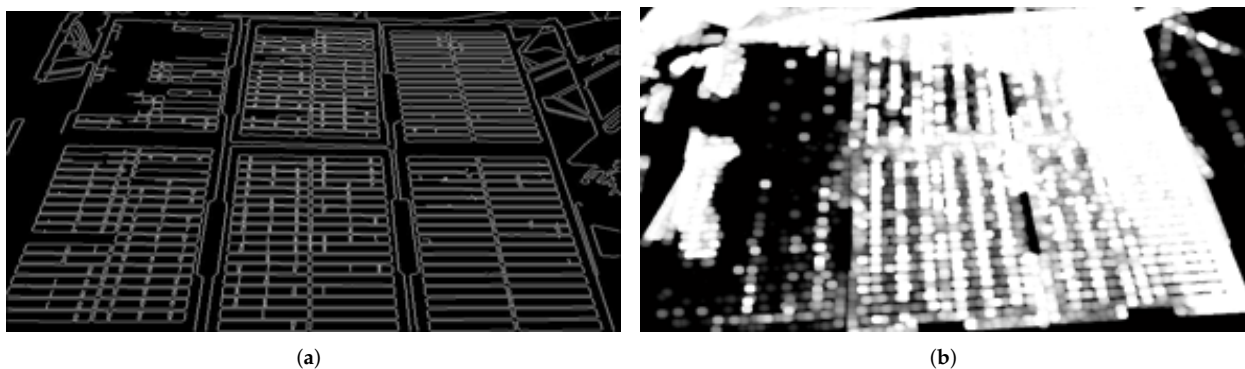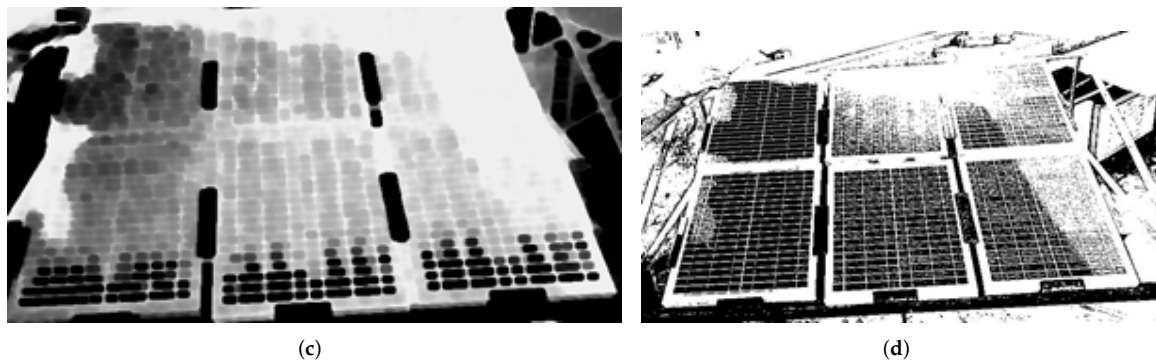

(a) (b)

Figure 2. *Cont.*

Figure 2. Image processing techniques in MALTAB libraries. (**a**) Canny Edge detection. (**b**) Morphed image. (**c**) Dilated image. (**d**) Black&White image.

2.3. Proposed Neighboring Pixel Algorithm (NPA)

To rectify the inherent issues of MATLAB-based libraries, a new algorithm, known as neighboring pixel algorithm (NPA), was devised as shown in Figure 3. The functional blocks of this flowchart are explained in the subsequent subsections. In this regard, Section 2.4 explains the image processing, whereas Section 2.5 explains the rest of the algorithm up to the GMPPT.
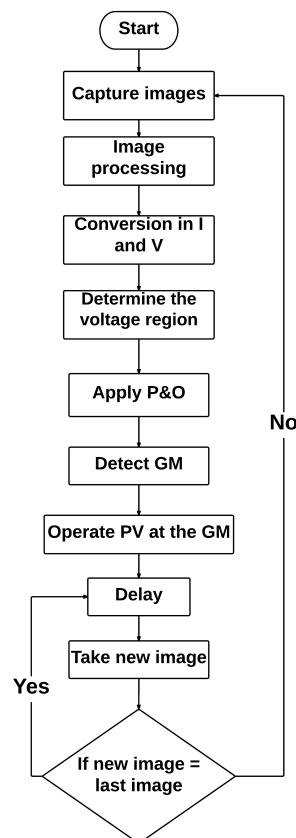
Figure 3. Flowchart of the proposed method.

In the proposed algorithm, images are continuously captured through an optical camera and are subsequently processed in MATLAB to detect the occurrence and nature of shade on PV panels. The proposed algorithm classifies a given PV image in terms of unshaded, lightly shaded and dark-shaded PV arrays. For this, the irradiation limit for shade classification is set as follows

- Unshaded PV module | 1000 $\frac{W}{m^2}$.

- Lightly shaded PV module | 500 $\frac{W}{m^2}$.
- Dark shaded PV module = 100 $\frac{W}{m^2}$.

These values of irradiance are manipulated in a PV array simulator to study the characteristics of PV arrays under a maximum number of possible shading scenarios. Thus, the shading patterns on a PV array are categorized as horizontal, vertical and diagonal. This classification method enables the proposed NPA to cover the maximum possibilities of shading combinations that can occur on a PV array.

2.4. Image Processing Workflow

The image processing workflow is shown in Figure 4. Here, an image I(x,y) represents the brightness or intensity of an image at pixel (x,y). The intensity value of an image ranges from [0–255], where typically 0 is considered black and 255 represent white. This implies that, to operate the shadow detection algorithm, the x-y values of each module is essential to classify the nature of the shadow. For this purpose, the *imshow* MATLAB command is utilized to read the image. Subsequent to this, the coordinates are determined by clicking the corner points of each module photo.

Note that the white crossings, which are actually tabbing ribbons, on the PV modules do not pose a problem in shadow detection as they have been found to cause a negligible effect on the accuracy of the proposed partial shading detection approach. The image is further processed by adjusting the saturation using the *imadjust* MATLAB command. Since the analysis is performed on a saturated grayscale image of each module, the percentage of pixels is determined at the module level. Moreover, the effect of image noise or camera reflection is also compensated for using the neighboring pixel concept.

This algorithm does a cross check to verify the imaging results because, due to bad image quality or faults in the captured image, some area in the image can be considered as partially shaded while they are actually unshaded. To take this fact into account, the proposed algorithm only considers those pixels as light/partially shaded, dark shaded or unshaded when the intensity of the neighboring pixels is within the same range, otherwise the image is considered as noise and is therefore ignored.

In this way, on the basis of the ratio of the number of pixels of partially shaded, fully shaded or unshaded pixels to the total number of pixels, modules are segregated as partially shaded, fully shaded or unshaded. These intensity ranges are assigned to the algorithm by pixel level intensity analysis in MATLAB, which shows the intensity value of each pixel in a particular area of image. Next, an equivalent pattern of a particular shading scenario is drawn to perform further mathematical analysis for determination of the GMPP region. The mathematical model of the proposed neighboring pixel algorithm is provided as (3)

$$
\begin{aligned}
V &= imread() \\
I &= rgb2gray(V) \\
I &= adjust(I, [0.2 \quad 0.37], [])
\end{aligned}
\tag{3}
$$

For detection of a fully shaded module:

$$
\begin{aligned}
D(i, j) &= 0 \\
D(i - 5, j) &= 0 \\
D(i + 5, j) &= 0
\end{aligned}
\tag{4}
$$

For detection of a partially shaded module:

$$
\begin{aligned}
40 &< L(i - 5, j) < 180 \\
40 &< L(i + 5, j) < 180 \\
40 &< L(i, j - 5) < 180 \\
40 &< L(i, j + 5) < 180
\end{aligned}
\tag{5}
$$

Similarly, the intensity range for unshaded modules is defined as (6)

$$220 < U(i - 5, j) < 255$$
$$220 < U(i + 5, j) < 255$$
$$220 < U(i, j - 5) < 255 \qquad (6)$$
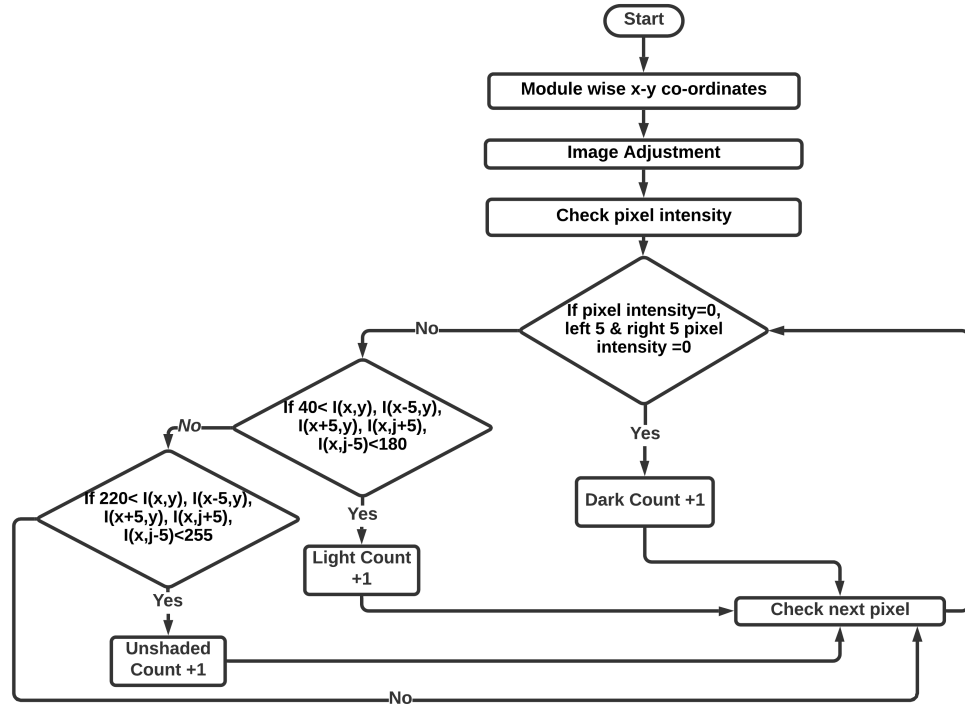$$220 < U(i, j + 5) < 255$$

Figure 4. Flowchart of the proposed image processing method.

2.5. Prediction of Maximum Voltage Region under Partial Shading Scenario

Prediction of the maximum voltage region under a partial shading scenario. The mathematical model predicts the voltage regions on the I-V curve of a PV array where the global maximum (GM) can appear. First, the I-V curve is divided into a number of regions equivalent to the series-connected modules (N_s) in a string. A consensus between scientists has been established that the number of local maxima (LMs) plus global maximum cannot exceed N_s, and the range of each voltage region is equal to the open-circuit voltage of module (V_{ocMod}). The value of V_{ocMod} can be estimated from the open-circuit voltage of array ($V_{ocArray}$):

$$V_{ocmod} = \frac{V_{ocarray}}{N_s} \qquad (7)$$

The mid-point voltage of each region is selected as a reference voltage (V_{Ref}), the mathematical representation of which is shown below

$$V_{Ref_n} = \sum_{n=1}^{N_s} \frac{V_{ocmod}}{2} + (n - 1) \times V_{ocmod} \qquad (8)$$

Using the V_{Ref} and I_{Ref} values of any two regions, their power values can be compared as indicated below

$$V_{Ref_n} \times I_{Ref_n} \leftrightarrow V_{Ref_n + x} \times I_{Ref_n + x} \qquad (9)$$

Here, the I_{Ref_n} of any region is equivalent to a combination of string currents, where the current of each string is estimated by the VI method according to the active/dominant

module of the string in that region. The currents of each string are assumed as unshaded/no-shade (NS) as I_{sc}, light-shaded (LS) as 50% of I_{sc} and dark-shaded (DS) as 10% of I_{sc}, as per the situation of the string detected by the VI method.

To elaborate the matter, consider a PV array composed of 5×3 ($N_s = 5$ and $N_p = 3$) modules. This means that five voltage regions take place where the currents of three strings are estimated by the VI method for each region. For instance, initially, the software compares the first and second region, where the V_{Ref} of the first and second regions comes out as $V_{ocMod}/2$ and $3V_{ocMod}/2$, respectively, from Equation (8).

Thereafter, the VI method declares that, in Region-1 (first region), the current scenario of three strings is as follows: the unshaded module of string-1 (I_{sc}) is active, the unshaded module of string-2 (I_{sc}) is active, and the light-shaded module of string-3 (50% I_{sc}) is active. Simultaneously, the VI method calculates the string currents in Region-2 (second region) as follows: the light-shaded module of string-1 (50% I_{sc}) is active, the dark-shaded module of string-2 (0.1% I_{sc}) is active, and the dark-shaded module of string-3 (0.1% I_{sc}) is active. Consequently, Equation (9) becomes

$$\frac{V_{ocmod}}{2} \times [I_{sc} + I_{sc} + I_{sc}] \leftrightarrow \frac{3V_{ocmod}}{2} \times [0.5I_{sc} + 0.5I_{sc} + 0.1I_{sc}] \tag{10}$$

This becomes

$$\frac{1}{2} \times [1 + 1 + 1] > \frac{3}{2} \times [0.5 + 0.1 + 0.1] \tag{11}$$

It can be seen that, since Region-1 exhibits the value of 1.5, which is higher than the 1.05 value of Region-2, Region-1 prevails and will be compared with Region-3 next. This comparison continues until all the regions are checked. Finally, the region that depicts the highest value as per Equation (9) will be declared as the GM region.

3. Concept Validation

The accuracy of the proposed image processing technique was verified through MATLAB as well as with a hardware prototype using the scheme shown in Figure 5. For the validation process, the PV arrays consisted of 3X2 SC20P-12 modules. The results of the image processing in the MATLAB simulation using the proposed method are presented in Figure 6. It can be seen that the proposed method reproduced the image in an efficient way.

Images were captured using a 16 MP commercially available point and shoot camera. The control algorithm was implemented using arduino ATmega328p. The PV array was connected to the battery load through a DC-DC boost converter with the following specifications

- Input capacitor (C_{in}) = 50 μF.
- Inductor (L) = 350 μH.
- Output capacitor (C_{out}) = 250 μF.
- Load = Battery of 48 V.
- Switching frequency f_s = 40 kHz.
- Scanning capacitor (C_{scan}) = 1 mF.

The guidelines for the designing the power electronic interface for PV applications can be found in [26–29]. The specifications of the PV module used for the PV array are tabulated in Table 1 [30].
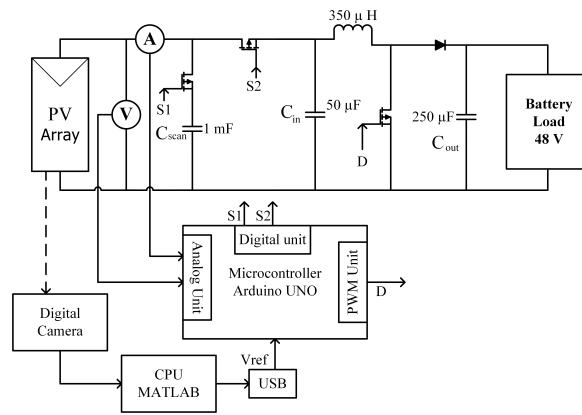
Figure 5. Concept validation scheme.

Table 1. Datasheet of the SC20P-12 PV module [30].

Parameters	Value
Maximum power (P_{mpp})	20 W
Voltage at maximum power (V_{mpp})	17.5 V
Current at maximum power (I_{mpp})	1.14 A
Open circuit voltage (V_{oc})	21.5 V
Short circuit current (I_{sc})	1.29 A

For concept validation, two artificial shades were created on the PV panels—named case 1 and case 2.
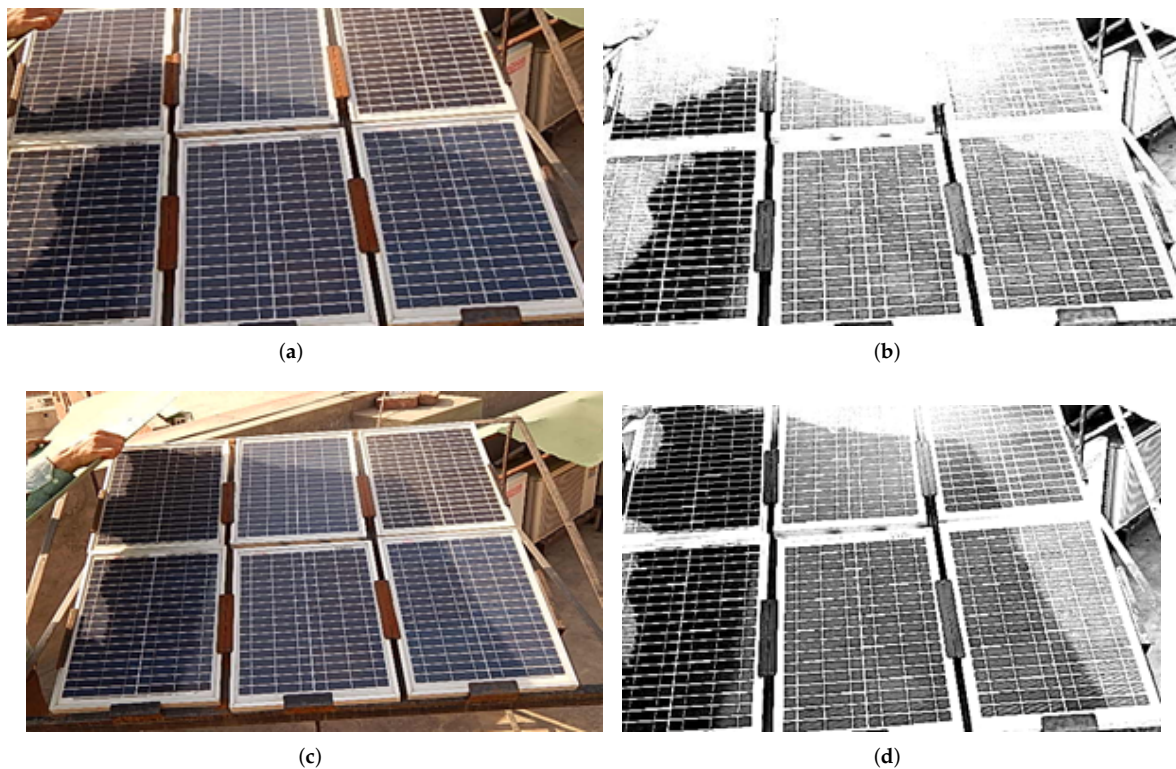

Figure 6. Image processing techniques in the MALTAB libraries. (**a**) Partial shading case 1, Actual image. (**b**) Case 1, Processed image. (**c**) Partial shading case 2, Actual image. (**d**) Case 2, Processed image.

For this purpose, testing was done on a 3 × 2 array while artificial shade was created on the PV panel.

3.1. Case 1

Initially, the image of the PV array was captured under partial shading. It was then processed to detect the shading scenario as shown in Figure 7.

| (a) | (b) |
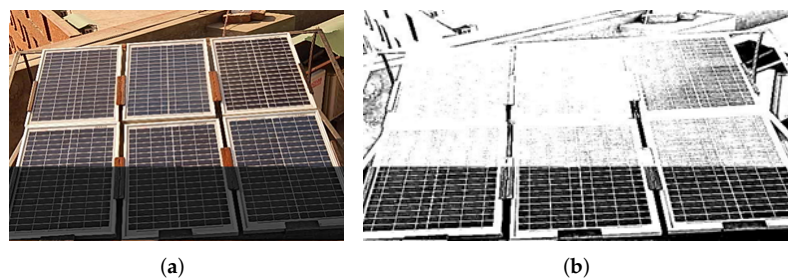
Figure 7. Image processing. (**a**) Partial shading case 1, hardware verification. (**b**) Processed image.

The mathematical model of the PV array under a shading scenario is

- A PV array consists of two series of connected modules where the V_{oc} of each module is 12 V. Therefore, two regions take place in the PV array, which are Region-1 (0–22 V) and Region-2 (22–44 V).
- The 11 and 33 V points are selected as the mid-points of Region-1 and Region-2, respectively.
- The VI method is engaged to determine the three strings situation in Region-1 and Region-2. The imaging method declares the following current values for strings in two regions:
  - Region-1: String-1 (S1) exhibits the 1.21 A, i.e., I_{sc}. This means that although S1 string is shaded but in Region-1, the current of the unshaded module prevails, while shaded modules are by-passed. The situation is the same with String-2 and String-3.
  - Region-2: The dark shaded module of each string is active as declared by the VI method. Consequently, the current value of each string is represented with a 10% I_{sc}, i.e., 0.121 A.

By comparing the powers of two regions, it is clear that the global maximum is present in Region-1. The proposed technique suggests that, for the present case, the MPP should occur in voltage Region-1 (1–22 V), and the reference voltage is 11 V. In order to validate the results of proposed technique, the I-V/P-V curves of the PV array were scanned under this partial shading scenario as shown in Figure 8. The results obtained from hardware were in accordance with the result, which was obtained from the proposed image processing technique. The technique further proposes the operating point of the PV array at the reference voltage and it is worth noticing that the actual GMPP exists at the reference voltage of Region1 of the PV array.
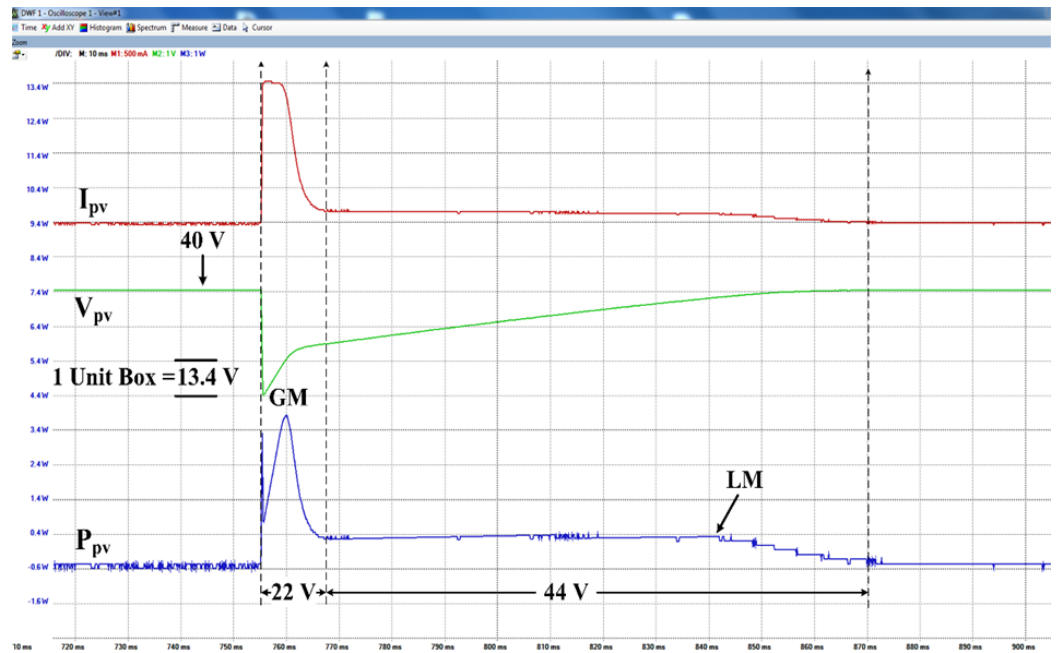
Figure 8. I-V and P-V under partial shading in case 1.

3.2. Case 2

For case 2, a different type of shade was created on the PV array, and the image was captured and further processed in MATLAB; Figure 9a,b. On the basis of the imaging results, an equivalent model was drawn to estimate the mathematical model for determination of the GMPP region. The proposed technique suggests that the MPP will be present in Region-2 (V_{Ref} = 33 V) under the current shading scenario. This is because of the reason that, in Region-1, all three strings are dominated by the current of the unshaded module, while in Region-2, only the S1 current is dictated by the dark-shaded module (10% I_{sc}), and the other modules are operating with unshaded modules. Naturally, the power of Region-2 is better in a power comparison of two regions. When the I-V/P-V curves were scanned, the GMPP was in Region-2, and the GMPP was at 33 V, which was in accordance with the proposed technique as shown in Figure 10.
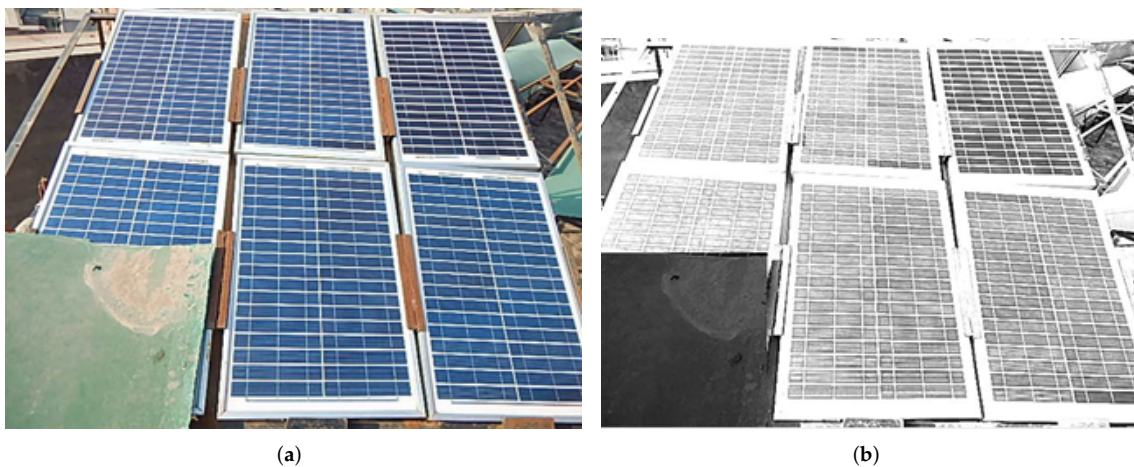

(**a**)   (**b**)

Figure 9. Image processing. (**a**) Partial shading case 2, hardware verification. (**b**) Processed image of case 2 of partial shading.
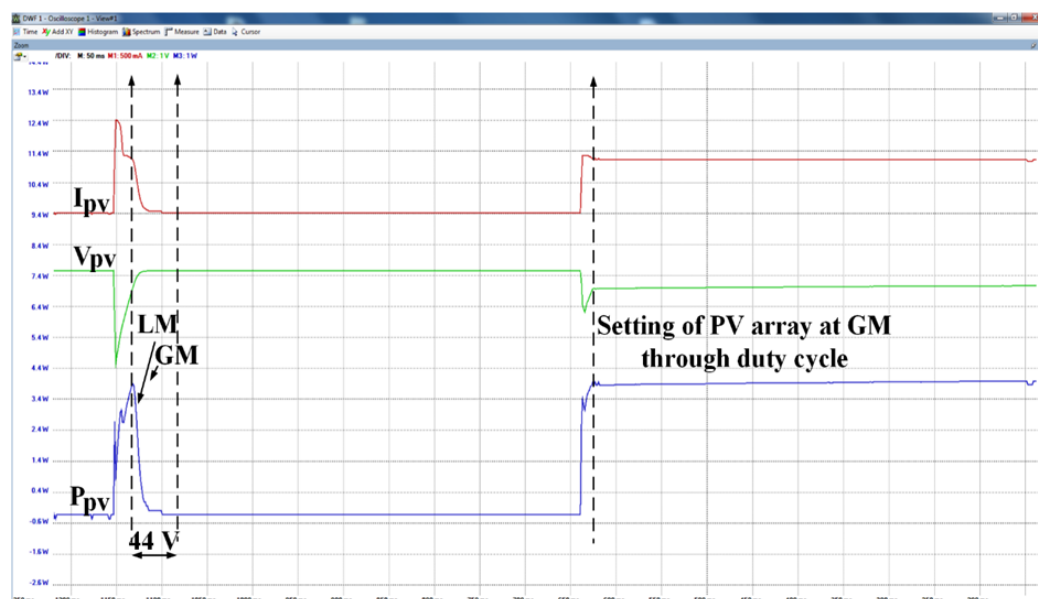
Figure 10. I-V and P-V under partial shading in case 2.

4. Conclusions

Artificial-intelligence-based MPPT methods are adaptive and can handle nonlinearities in a PV system. The striking feature of these techniques is that there is no need to isolate the load from photovoltaic. Operation of a PV at the maximum power point can be ensured without scanning the I-V/ P-V curves. Moreover, only simplified mathematical models are required, and no expensive sensors are needed for implementation of these techniques. These techniques can be implemented in both standalone and grid-connected PV systems.

These techniques can also be integrated with existing MPPT techniques. The proposed technique detects the shaded portion of a PV array after capturing the image by further performing image processing techniques. Later, the results obtained from image processing are utilized to manipulate the values of the current in power equations. In this way, the MPP region is determined. Finally, the PV array is designed to set on the reference voltage of the determined voltage region through a demodulation scheme.

The proposed scheme was tested both through hardware and software simulations on a 3×2 sized PV plant. The hardware results were in accordance with the results achieved from proposed image processing technique. The proposed technique is cost effective as it utilizes a simple optical camera as compared to an infrared camera to detect and classify shading on a PV plant.

We observed that the results of the proposed technique contained less uncertainty in the case of low-resolution images, whereas the level of uncertainty increased when high-resolution images were tested. This is likely caused by the small image details that are taken into account when images are captured from a high-resolution lens. The proposed algorithm can be further improved in order to minimize the extent of uncertainty in the case of high resolution images by exploring more advanced image processing techniques.

Author Contributions: Conceptualization, H.R. and A.F.M.; methodology, A.F.M. and H.A.S.; software, A.M.N.; validation, H.R., A.F.M., H.A.S. and A.A.A.-S.; formal analysis, A.F.M.; investigation, A.A.A.-S.; resources, A.M.N.; data curation, A.M.N.; writing—original draft preparation, H.A.S.; writing—A.A.; visualization, A.F.M.; supervision, F.S.; project administration, A.A.; funding acquisition, A.A. All authors have read and agreed to the published version of the manuscript.

Data Availability Statement: No new data were created or analyzed in this study. Data sharing is not applicable to this article.

Conflicts of Interest: The authors declare no conflict of interest.

References

1. Lewis, N.S. Toward cost-effective solar energy use. *Science* **2007**, *315*, 798–801. [CrossRef]
2. Sher, H.A.; Murtaza, A.F.; Addoweesh, K.E.; Chiaberge, M. Pakistan's progress in solar PV based energy generation. *Renew. Sustain. Energy Rev.* **2015**, *47*, 213–217. [CrossRef]
3. Li, Y.; Wang, J.; Wang, R.; Gao, D.W.; Sun, Q.; Zhang, H. A Switched Newton-Raphson-Based Distributed Energy Management Algorithm for Multienergy System Under Persistent DoS Attacks. *IEEE Trans. Autom. Sci. Eng.* **2021**, 1–13. [CrossRef]
4. Sher, H.A.; Murtaza, A.F.; Addoweesh, K.E.; Chiaberge, M. An intelligent off-line MPPT technique for PV applications. In Proceedings of the 2013 IEEE Conference on Systems, Process & Control (ICSPC), Kuala Lumpur, Malaysia, 13–15 December 2013; pp. 316–320.
5. Ahmad, R.; Murtaza, A.F.; Sher, H.A.; Shami, U.T.; Olalekan, S. An analytical approach to study partial shading effects on PV array supported by literature. *Renew. Sustain. Energy Rev.* **2017**, *74*, 721–732. [CrossRef]
6. Sher, H.A.; Murtaza, A.F.; Al-Haddad, K. A hybrid maximum power point tracking method for photovoltaic applications with reduced offline measurements. In Proceedings of the 2017 IEEE International Conference on Industrial Technology (ICIT), Toronto, ON, Canada, 22–25 March 2017; pp. 1482–1485.
7. Shams, I.; Mekhilef, S.; Tey, K.S. Improved-Team-Game-Optimization-Algorithm-Based Solar MPPT With Fast Convergence Speed and Fast Response to Load Variations. *IEEE Trans. Ind. Electron.* **2020**, *68*, 7093–7103. [CrossRef]
8. Murtaza, A.F.; Sher, H.A.; Spertino, F.; Ciocia, A.; Noman, A.M.; Al-Shamma'a, A.A.; Alkuhayli, A. A Novel MPPT Technique Based on Mutual Coordination between Two PV Modules/Arrays. *Energies* **2021**, *14*, 6996. [CrossRef]
9. Murtaza, A.F.; Sher, H.A.; Al-Haddad, K.; Spertino, F. Module level electronic circuit based PV array for identification and reconfiguration of bypass modules. *IEEE Trans. Energy Convers.* **2020**, *36*, 380–389. [CrossRef]
10. Shams, I.; Mekhilef, S.; Tey, K.S. Maximum power point tracking using modified butterfly optimization algorithm for partial shading, uniform shading, and fast varying load conditions. *IEEE Trans. Power Electron.* **2020**, *36*, 5569–5581. [CrossRef]
11. Ahmad, R.; Murtaza, A.F.; Sher, H.A. Power tracking techniques for efficient operation of photovoltaic array in solar applications—A review. *Renew. Sustain. Energy Rev.* **2019**, *101*, 82–102. [CrossRef]
12. Anh, D.T. Autonomous Solar Panel Cleaner with Image Processing and Neural Network. Ph.D. Thesis, Vietnamese-German University, Thu Dau Mot, Vietnam, 2021.
13. de Carvalho Neto, J.T. Qualitative and Quantitative Diagnostic Device for Detecting Defects in Crystalline Silicon PV Cells. *IEEE Trans. Device Mater. Reliab.* **2021**, *21*, 647–657. [CrossRef]
14. Hu, Y.; Cao, W.; Wu, J.; Ji, B.; Holliday, D. Thermography-based virtual MPPT scheme for improving PV energy efficiency under partial shading conditions. *IEEE Trans. Power Electron.* **2014**, *29*, 5667–5672. [CrossRef]
15. Guerriero, P.; Cuozzo, G.; Daliento, S. Health diagnostics of PV panels by means of single cell analysis of thermographic images. In Proceedings of the 2016 IEEE 16th International Conference on Environment and Electrical Engineering (EEEIC), Florence, Italy, 7–10 June 2016; pp. 1–6.
16. Karakose, M.; Baygin, M. Image processing based analysis of moving shadow effects for reconfiguration in PV arrays. In Proceedings of the 2014 IEEE International Energy Conference (ENERGYCON), Cavtat, Croatia, 13–16 May 2014; pp. 683–687.
17. Mahmoud, Y.; El-Saadany, E.F. A Novel MPPT Technique Based on an Image of PV Modules. *IEEE Trans. Energy Convers.* **2017**, *32*, 213–221. [CrossRef]
18. Aghaei, M.; Grimaccia, F.; Gonano, C.A.; Leva, S. Innovative Automated Control System for PV Fields Inspection and Remote Control. *IEEE Trans. Ind. Electron.* **2015**, *62*, 7287–7296. [CrossRef]
19. Vergura, S.; Marino, F. Quantitative and Computer-Aided Thermography-Based Diagnostics for PV Devices: Part I 8212; Framework. *IEEE J. Photovoltaics* **2017**, *7*, 822–827. [CrossRef]
20. Vergura, S.; Colaprico, M.; de Ruvo, M.F.; Marino, F. A Quantitative and Computer-Aided Thermography-Based Diagnostics for PV Devices; Part II: Platform and Results. *IEEE J. Photovoltaics* **2017**, *7*, 237–243. [CrossRef]
21. Marschner, S.R.; Westin, S.H.; Lafortune, E.P.; Torrance, K.E. Image-based bidirectional reflectance distribution function measurement. *Appl. Opt.* **2000**, *39*, 2592–2600. [CrossRef]
22. McAndrew, A. An introduction to digital image processing with matlab notes for scm2511 image processing. *Sch. Comput. Sci. Math. Vic. Univ. Technol.* **2004**, *264*, 1–264.
23. Hussain, A.; Sher, H.A.; Murtaza, A.F.; Al-Haddad, K. Improved restricted control set model predictive control (iRCS-MPC) based maximum power point tracking of photovoltaic module. *IEEE Access* **2019**, *7*, 149422–149432. [CrossRef]
24. Shams, I.; Mekhilef, S.; Tey, K.S. Improved Social Ski Driver-Based MPPT for Partial Shading Conditions Hybridized with Constant Voltage Method for Fast Response to Load Variations. *IEEE Trans. Sustain. Energy* **2021**, *12*, 2255–2267. [CrossRef]
25. Seritan, G.C.; Enache, B.A.; Adochiei, F.C.; Argatu, F.C.; Christodoulou, C.; Vita, V.; Toma, A.R.; Gandescu, C.H.; Hathazi, F.I. Performance evaluation of photovoltaic panels containing cells with different bus bars configurations in partial shading conditions. *Rev. Roum. Sci. Tech.-Ser. Electrotech. Energetique* **2020**, *65*, 67–70.

26. Xiao, W.; Ozog, N.; Dunford, W.G. Topology study of photovoltaic interface for maximum power point tracking. *IEEE Trans. Ind. Electron.* **2007**, *54*, 1696–1704. [CrossRef]

27. Sher, H.A.; Addoweesh, K.E.; Al-Haddad, K. Performance enhancement of a flyback photovoltaic inverter using hybrid maximum power point tracking. In Proceedings of the IECON 2015—41st Annual Conference of the IEEE Industrial Electronics Society, Yokohama, Japan, 9–12 November 2015; pp. 005369–005373.

28. Kim, Y.H.; Jang, J.W.; Shin, S.C.; Won, C.Y. Weighted-efficiency enhancement control for a photovoltaic AC module interleaved flyback inverter using a synchronous rectifier. *IEEE Trans. Power Electron.* **2014**, *29*, 6481–6493. [CrossRef]

29. Zhang, L.; Hu, H.; Feng, L.; Xing, Y.; Ge, H.; Sun, K. A weighted efficiency enhancement control for modular grid-tied photovoltaic generation system. In Proceedings of the IECON 2011—37th Annual Conference of the IEEE Industrial Electronics Society, Melbourne, VIC, Australia, 7–10 November 2011; pp. 3093–3098.

30. SC20P-12 Solar PV Module Datasheet. Available online: https://www.enfsolar.com/pv/panel-datasheet/crystalline/14019 (accessed on 16 January 2022).